Quantum Confinement and Nonlinear Optical Response of Conjugated Molecules

H.X. Wang, A. Takahashi, M. Hartmann and S. Mukamel

Department of Chemistry, University of Rochester, Rochester, NY 14627

(January 20,1993)

The nonlinear optical response (NLO) of linear polyenes and fullerenes is studied using an anharmonic oscillator model. The influence of size effects and quantum exciton confinement on the nonlinear optical response is examined, and the time evolution of the excitons is studied. The elementary optical excitations for C_{60} are shown to be correlated charge density fluctuations. For linear polyenes with finite size, oscillations in the time-resolved degenerated four wave mixing (D4WM) signal due to the coherent excitation of several band states are found within the Hückel model (no Coulomb interaction). For infinite size a photon echo like behaviour is obtained. The exciton–exciton interaction changes the lineshape of the D4WM signal and gives rise to a broad delayed signal whose position is given by the dephasing time of the system.

I. INTRODUCTION

Molecules with large electronic nonlinear polarizabilities are of great interest for nonlinear optical applications.[1–3] Optical nonlinearities of materials with delocalized valence electrons are enhanced in systems with reduced dimension (quantum well structures, quantum wires, quantum dots), where the valence electrons are confined in regions shorter than their natural delocalization length in the bulk. The magnitude of the off-resonant NLO response, which is most relevant for the practical use of these materials, and its scaling with size had received a considerable attention.[4–7] In addition to the reduced dimensionality, the NLO response depends on the size of the polyene. A power scaling law on molecular size $\chi^{(3)} \sim N^b$ has been established,[5] N being the number of the double bonds. The scaling is expected to saturate for large N where the thermodynamic limit implies that $b = 1$. Such saturation for the Hückel model and the Pariser–Parr–Pople (PPP) model has been studied.[6,8–10] The Coulomb interaction leads to the formation of excitonic states. Calculations of the linear and nonlinear optical response have demonstrated that the excitons have an intermediate character between Frenkel and Wannier type.[11] The optical transitions, oscillator strength and exciton dynamics have been shown to depend on the quantum confinement of the excitons.[12,13] The response time, one of the other necessary requests for nonlinear optical materials, is also determined by the elementary excitations of the system.[14]

Much effort have been made towards measuring and calculating the off-resonant $\chi^{(3)}$ of C_{60} molecules.[15,16] Experimentally, the third harmonic generation (THG) and the degenerate four wave mixing (D4WM) techniques have resulted in a third order polarizability comparable to that of polydiacetylenes. Theoretical modeling has been primarily based on the free electron (Hückel) model. We have studied the absolute magnitude and dispersion of the third order susceptibility of C_{60} using the time-dependent Hartree Fock (TDHF) method.[13] The importance of long-range Coulomb interaction which leads to the formation of excitons has been established.[1,8,10,13,17]

In this paper we investigate the effects of quantum confinement, exciton dynamics and the interactions among excitons on the NLO response of conjugated molecules. We consider the static, frequency dispersed, and time-resolved four wave mixing spectroscopy which are powerful methods for studying elementary excitations in solids.[14,18] Starting with the PPP model, we solve the problem using a density matrix approach and two approximations for closing the many-body hierarchy, the coherent wave approximation (CWA), and the TDHF. The renormalization of the ground state due to the Coulomb interaction and molecule-field interactions are included nonperturbatively. We demostrate the advantages of utilizing a two-band approach[8,12,19,20] instead of using individual molecular eigenstates. Our approach focuses directly on the elementary excitations (electron–hole pairs) and can be easily applied to large sizes. The effects of exciton dynamics can be clearly accounted for. Both the frequency dispersed and the time-resolved NLO response can be studied in a unified manner. For linear polyenes, we find the excitons to be extended over 20 double bonds and the saturation size of $\chi^{(3)}$ is closely related to the exciton size. The interactions between excitons give a delayed response in the time-resolved D4WM. In a C_{60} molecule we find exciton like characteristic collective motions. These excitons are very similar in shape in each order of the field for all frequencies studied. The amplitudes of these collective motions strongly depend on the frequencies and are responsible for the linear and

nonlinear polarizabilities.

In Sec. II we give a brief summary of the model. In Sec. III we derive the equation of motion for the density matrix in the site representation and discuss different factorization procedures to close the equation of motion. In Sec. IV we present our numerical calculations for size scaling of nonlinear optical response. In Sec. V we study the time resolved D4WM. Finally, we present the NLO response of C_{60} in Sec. VI.

II. MODEL HAMILTONIAN

Our study starts with the PPP Hamiltonian for the π-electrons,

$$H = H_0 + H^{'} + H_{\rm int} \,. \tag{1}$$

The first term, H_0, is the Hückel Hamiltonian

$$H_0 = \sum_{n,m,\sigma} t_{m,n} \hat{\rho}^{\sigma}_{n,m} \tag{2}$$

where $t_{m,n}$ is the hopping integral between the n'th and m'th sites and $\hat{\rho}$ is the binary electron operator defined as $\hat{\rho}^{\sigma}_{n,m} = c^{\dagger}_{m,\sigma} c_{n,\sigma}$. $c^{\dagger}_{n,\sigma}(c_{n,\sigma})$ creates (annihilates) a π-electron of spin σ at the n'th site and they satisfy the anticommutation relation $[c^{\dagger}_{m,\sigma}, c_{n,\sigma'}]_+ = \delta_{m,n}\delta_{\sigma,\sigma'}$. The nearest-neighbour hopping integral is denoted as $t_{m,n} = \beta(1+\delta)$ for double bonds and $t_{m,n} = \beta(1-\delta)$ for single bonds. Otherwise $t_{m,n} = 0$. β and δ are the two parameters in the Hückel model. The second term $H^{'}$ in Eq. (1) describes the electron–electron Coulomb interaction

$$H^{'} = \sum_{n} U \hat{\rho}^{\uparrow}_{n,n} \hat{\rho}^{\downarrow}_{n,n} + \frac{1}{2} \sum_{n,m,\sigma,\sigma'}^{n \neq m} V_{n,m} \hat{\rho}^{\sigma}_{n,n} \hat{\rho}^{\sigma'}_{m,m} \tag{3}$$

where the repulsion $V_{n,m}$ between the n'th and m'th sites is given by Ohno's formula as

$$V_{n,m} = \frac{U}{\sqrt{1 + (r_{n,m}/a_0)^2}}. \tag{4}$$

The on-site Hubbard repusion U is given by $U = U_0/\varepsilon$. $U_0 = 11.13$ eV is the unscreened on-site repulsion, ε is the dielectric constant, and $a_0 = 1.2935\mathring{A}$. The dielectric constant $\varepsilon = 1$ is appropriate for short polyenes but $\varepsilon = 2$ is appropriate for long polyenes due to the screening by the σ electrons. Since both the Hamiltonian and the static Hartree–Fock ground state are symmetric with respect to spin exchange, the TDHF solution must also have this symmetry. We thus omit the spin index hereafter, and define $\hat{\rho} \equiv \hat{\rho}^{\uparrow} = \hat{\rho}^{\downarrow}$.

The third term $H_{\rm int}$ in Eq. (1) is the interaction Hamiltonian between the π electrons and the external laser field $E(t)$, which is polarized along the chain (z) axis for a linear polyene and along the axis vertical to one of the pentagons for C_{60}. Within the dipole approximation, it is given by $H_{int} = -E(t)\hat{P}$. $\hat{P}$ is the total polarization operator of a molecule given by

$$\hat{P} \equiv -2e \sum_{n} z(n) \hat{\rho}_{n,n}. \tag{5}$$

$-e$ is the electron charge and $z(n)$ is the z-coordinate of the n'th site. Since the optical wavelength is much longer than the size of the molecules to be considered, we take $E(t)$ to be uniform.

III. EQUATIONS OF MOTION

We assume that the state of the molecule at time t is described by the wave function $|\Psi(t)\rangle$. From the Schrödinger equation, the expectation value of the binary electron operator $\rho_{n,m}(t) = \langle\Psi(t)|\hat{\rho}_{n,m}|\Psi(t)\rangle \equiv \langle\hat{\rho}_{n,m}(t)\rangle$ is given by

$$i\hbar\dot{\rho}_{n,m}(t) = \langle\Psi(t)|[\hat{\rho}_{n,m}, H]|\Psi(t)\rangle. \tag{6}$$

The expectation values $\rho_{n,m}$ can be interpreted as elements of the single electron density matrix. Utilizing the commutation relations, we can calculate the right-hand side of these equations, and obtain

$$\begin{aligned} i\hbar\dot{\langle\hat{\rho}_{n,m}\rangle}(t) = &\sum_i \{t_{n,i}\langle\hat{\rho}_{i,m}\rangle - t_{i,m}\langle\hat{\rho}_{n,i}\rangle\} + U\{\langle\hat{\rho}_{n,n}\hat{\rho}_{n,m}\rangle - \langle\hat{\rho}_{m,m}\hat{\rho}_{n,m}\rangle\} \\ &+ e\{z(n) - z(m)\}E(t)\langle\hat{\rho}_{n,m}\rangle + \sum_{i,i\neq n} V_{n,i}\{\langle\hat{\rho}_{i,i}\hat{\rho}_{n,m}\rangle + \langle\hat{\rho}_{n,m}\hat{\rho}_{i,i}\rangle\} \\ &- \sum_{i,i\neq m} V_{m,i}\{\langle\hat{\rho}_{i,i}\hat{\rho}_{n,m}\rangle + \langle\hat{\rho}_{n,m}\hat{\rho}_{i,i}\rangle\}. \end{aligned} \tag{7}$$

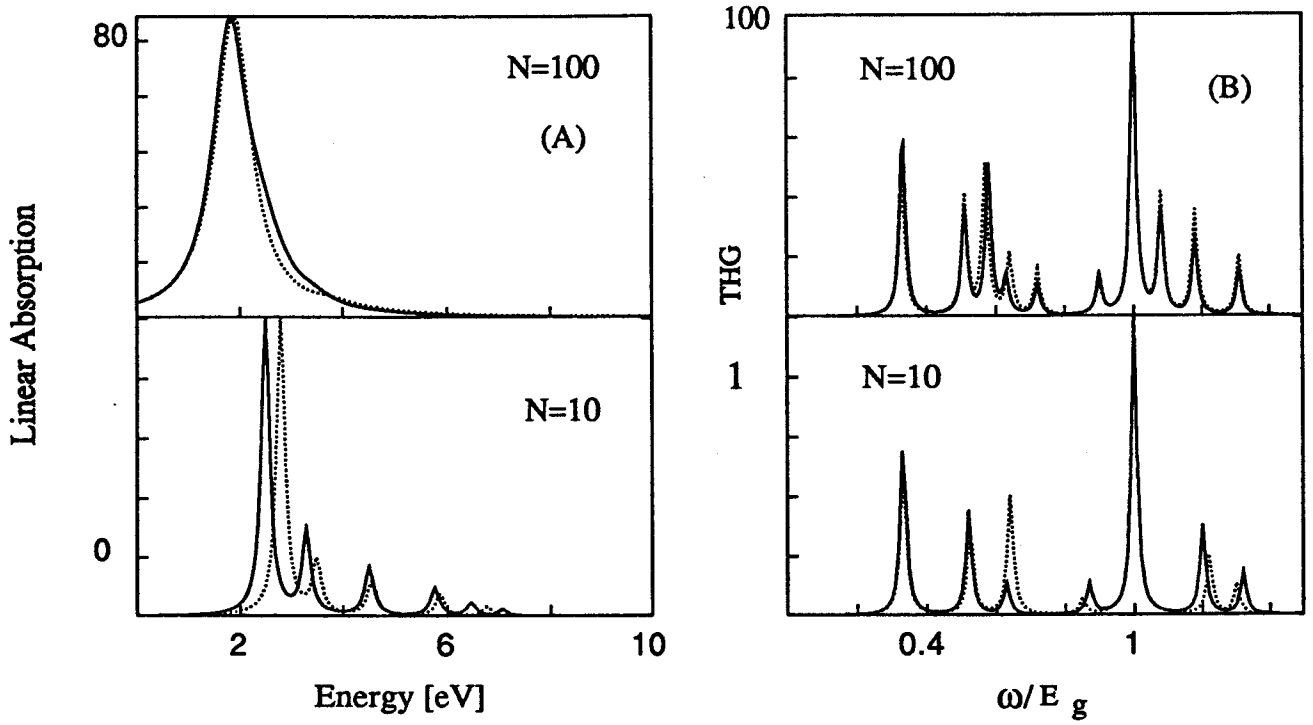

FIG. 1. Absorption (A) and third harmonic generation (B) for polyacetylene $\delta = 0.07$, $\beta = 2.4$, $U = 11.13eV$. top panel $N = 100$; bottom panel $N = 10$. Solid-CWA; Dotted-TDHF.

These equations of motion are exact, but they are not closed; they contain new higher order variables $\langle\hat{\rho}_{n,m}\hat{\rho}_{n_1,m_1}\rangle$ on the right hand side. We have used different factorization approximations to close the hierarchy. In the TDHF approximation[13] we assume that the wavefunction $|\Psi(t)\rangle$ is given by a single Slater determinant for all times. Thus we factorize the product of four operators as[21]

$$\langle c_m^\dagger c_n c_{m_1}^\dagger c_{n_1}\rangle = \langle c_m^\dagger c_n\rangle\langle c_{m_1}^\dagger c_{n_1}\rangle + \langle c_m^\dagger c_{n_1}\rangle\langle c_n c_{m_1}^\dagger\rangle, \tag{8}$$

and obtain closed equations of motion for the density matrix

$$i\hbar\dot{\rho}(t) = [h(t) + f(t), \rho(t)], \tag{9}$$

where $h(t)$ is the Fock operator matrix of $H_0 + H'$, and f is the Fock operator matrix of $H_{\rm int}$. In the limit $f \to 0$, the TDHF equation reduced to the random phase approximation (RPA) equation. The RPA method takes into account small amplitude quantum fluctuations around the static mean field solution and describes small amplitude collective motions very well. Since we solve the TDHF equation in powers of the external field, we also incorporate the coupling of the RPA modes. Thus large amplitude fluctuations can be described.

On the other hand, in the CWA which was derived using the Wannier representation , the electron operator products $\langle c_m^\dagger c_n c_{m_1}^\dagger c_{n_1}\rangle$ are factorized as[10,12]

$$\langle c_m^\dagger c_n c_{m_1}^\dagger c_{n_1}\rangle = \langle c_m^\dagger c_n\rangle\langle c_{m_1}^\dagger c_{n_1}\rangle + \delta_{n_1,m}\langle c_n c_{m_1}^\dagger\rangle - \delta_{m,n}\langle c_{m_1}^\dagger c_{n_1}\rangle. \tag{10}$$

With these factorizations we keep the minimum set of relevant variables necessary for calculating the polarization. The resulting equations map the calculation onto the dynamics of $N(2N-1)$ coupled anharmonic oscillators.[12]

We have calculated the linear absorption Fig. (1)(a) and third harmonic generation Fig. (1)(b) for polyacetylene using both the CWA and the TDHF approximations. Both methods give qualitatively similar spectra and the differences become smaller for larger sizes.

IV. SIZE SCALING OF NONLINEAR SUSCEPTIBILITIES

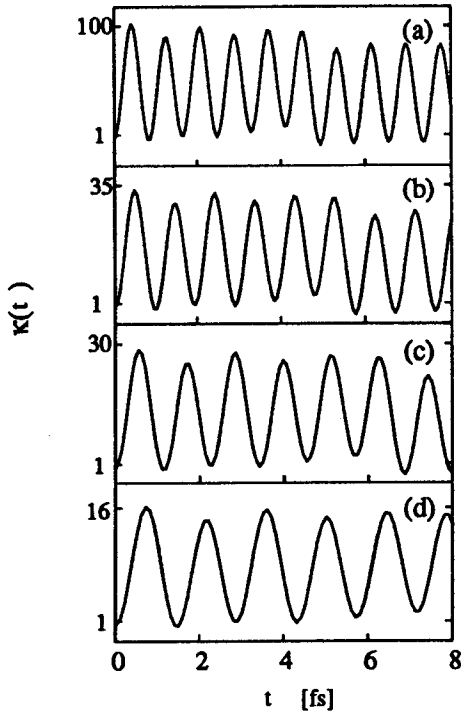

FIG. 2. The inverse participation ratio $\kappa(t)$ for polyacetylene ($\delta = 0.07$) and different values of the Hubbard interaction magnitude U. (a) $U = 0eV$, (b) $U = 4eV$, (c) $U = 8eV$, (d) $U = 11.13eV$.

The time evolution of an electron-hole pair following an impulsive (very short) excitation pulse at $t = 0$ is a direct measure of the nature of the excitons. When the polyene is small compared with the optical wavelength, the initial excitation is uniform (k=0). The probability $P_s(t)$ of the pair to be separated by s lattice units at time t is determined by the Green function for the electron-hole pair[10].

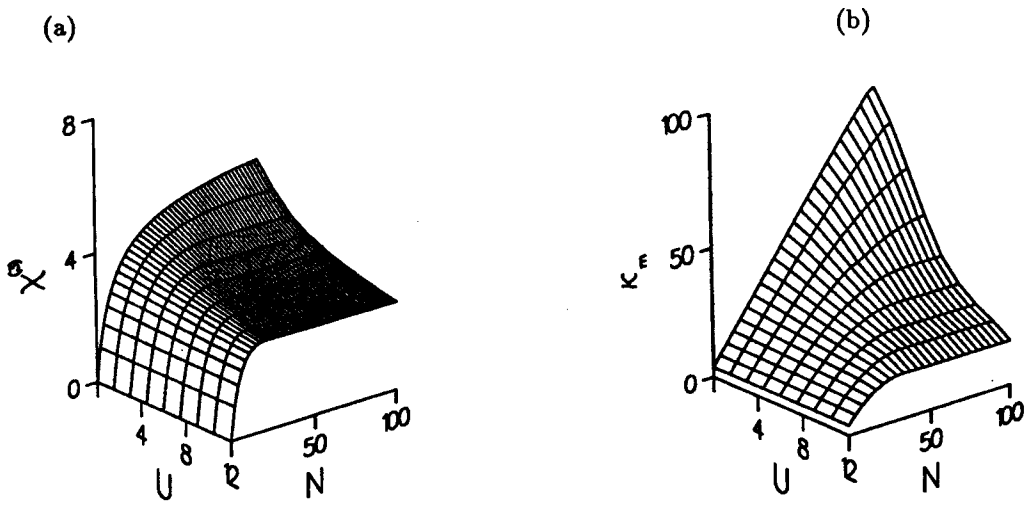

FIG. 3. The variation of the static susceptibility (a) $\chi^{(3)}(0)$ and κ_m (b) for polyacetylene ($\delta = 0.07$) with molecular size N and Hubbard interaction U.

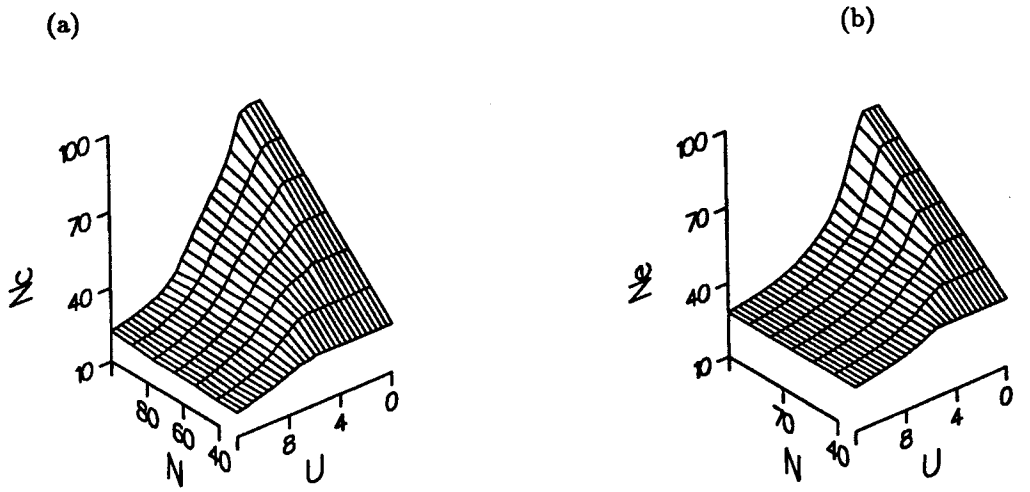

FIG. 4. The variation of the coherence size (a) N_c associated with $\chi^{(3)}$ and (b) N_e associated with κ_m with molecular size N and Hubbard interaction U.

A useful measure for the delocalization of the electron–hole pair is the *inverse participation ratio*[10,22] $\kappa(t) \equiv 1/\sum_s P_s^2(t)$. If the pair is separated over M sites then $P_s(t) \sim M^{-1}$ and therefore $\kappa \sim M$. In Fig. 2 we display the variation of $\kappa(t)$ with time for different values of the Coulomb interaction ranging from $U = 0$ (Hückel model) to 11.13 eV for polyacetylene with $N = 100$ double bonds. In all cases the electron and the hole are created on the same bond so that initially $\kappa(0) \sim 1$ independent of the Coulomb interaction strength. The subsequent evolution is however very different. For the Hückel model ($U = 0$, panel (a)) the pair is uncorrelated and $\kappa(t)$ oscillates between 1 and the polyene size 100. As U is increased in the following panels, the electron and the hole become tightly bound (localized) and the maximum s value (i.e. the exciton delocalization length) decreases. The figure thus clearly illustrates the formation of charge-transfer bound excitons which become more tightly bound with increasing U. Fig. (3)(a) demonstrates how the saturation of $\chi^{(3)}(0)$ occurs at smaller sizes N as U increases. In Fig. (3)(b) we display the variation of the amplitude κ_m of the $\kappa(t)$ oscillation with N and U. The slope of the curves in Fig. (3) drops abruptly to 1 at a critical size.[8,10] We define that point as the nonlinear coherence size N_c related to the static $\chi^{(3)}$ and exciton coherence size N_e related to κ_m. The dependence of N_c and N_e on molecule size N and Hubbard

interaction U is displayed in Fig. (4) The remarkable correlation between N_c and N_e in Fig. (4) firmly establishes that the scaling and saturation of $\chi^{(3)}$ with molecular size closely resembles the exciton coherence-size associated with the relative electron-hole motion.

V. TIME RESOLVED NONLINEAR OPTICAL RESPONSE

The delocalization of the electron-hole pair can be explored using time-resolved nonlinear optical spectroscopy. In the simplest of these techniques two laser pulses propagating along the directions $\vec{k}_1$ and $\vec{k}_2$, generate a transient polarization grating which diffracts photons into the direction $2\vec{k}_1 - \vec{k}_2$. This technique was applied to study the dephasing of molecular systems and semiconductors observing quantum beats of excitons[23,25], photon echos[26,27] and coherent interactions of excitons resulting in characteristic D4WM signals.[28] The calculation of the D4WM signal can be appropriately performed using a two band model (valence band v and conduction band c). The corresponding equation of motion for the density matrix Eq. (7) can be written in Bloch function representation (wave vector K).[14] Here we will briefly discuss the structure of the system of equations. A strong pump field $E_1(\vec{k}_1, t)$ propagates in the direction of $\vec{k}_1$ and a weak probe field $E_2(\vec{k}_2, t)$ which is time delayed τ with respect to the pump field propagates in the direction $\vec{k}_2$. We assume that both pulses are polarized in the direction of the chain of the linear polyene. The exciting pump field gives rise to a renormalized *ground state* characterized by the one-particle distributions $n_K(t)$ and polarization $\psi_K(\vec{k}_1, t)$, while the linear response to the probe field $\delta\psi_K(\vec{k}_2, t)$ contains the information about the renormalized *excitation spectra*. Furthermore one obtains a diffracted polarization $\delta\psi_K(\vec{k}_s, t)$ resulting from the diffraction of the pump off the grating generated by the interference with the probe and propagating in the direction of $\vec{k}_s = 2\vec{k}_1 - \vec{k}_2$. From this diffracted polarization one can determine the time–resolved D4WM signal as

$$S(\vec{k}_s, t) \equiv |\sum_K \delta\psi_K(\vec{k}_s, t)|^2. \tag{11}$$

The equation for the diffracted polarization reads

$$\begin{aligned}
&\{-i\hbar\frac{\partial}{\partial t} - i\gamma - (\varepsilon_{cK} - \varepsilon_{vK}) + 2\Delta_K(t)\}\delta\psi_K(\vec{k}_s, t) \\
&+ (1 - 2n_K(t))\delta\Omega_K(\vec{k}_s, t) = 2\delta n_K(\vec{k}_1 - \vec{k}_2, t)\Omega_K^*(\vec{k}_1, t) \\
&- 2\psi_K^*(\vec{k}_1, t)\delta\Delta_K(\vec{k}_1 - \vec{k}_2, t)
\end{aligned} \tag{12}$$

where γ is a transverse damping constant. The diffracted polarization is driven by the Rabi frequency $\Omega_K(\vec{k}_1, t) = \mu_K E_1(\vec{k}_1, t) + \sum_{K'} V_{K-K'}\psi_{K'}(\vec{k}_1, t)$ which contains local field corrections to the external field due to the Coulomb interaction of the electrons in the conduction and valence band. V_K is the Fourier transform of Ohno's potential (4) and μ_K is the interband dipole moment. Furthermore the Coulomb interaction leads to a renormalization of the Hartree-Fock single particle energies ε_{cK} and ε_{vK} of the conduction and valence band, respectively, expressed by the self energy $\Delta_K(t)$. There are two nonlinear terms in the equation. The population $n_K(t)$ entering the last term of the LHS of Eq. (12) takes into account the Pauli exclusion principle. $\delta\Omega_K$ accounts for the change of the local field due to the probe pulse. The other nonlinear process is the diffraction of the pump pulse, which enters in Ω_K and ψ_K on the RHS of Eq. (12), off the grating created by the interference of pump and probe described by δn_K and $\delta\Delta_K$. Because this contribution is proportional to the Coulomb interaction (contained in Ω_K and $\delta\Delta_K$), this nonlinear process represents exciton-exciton interaction. The complete system of equations determining the diffracted polarization includes those for the quantities $n_K(t), \psi_K(\vec{k}_1, t), \delta\psi_K(\vec{k}_2, t)$ and $\delta n_K(\vec{k}_1 - \vec{k}_2, t)$.[14,28]

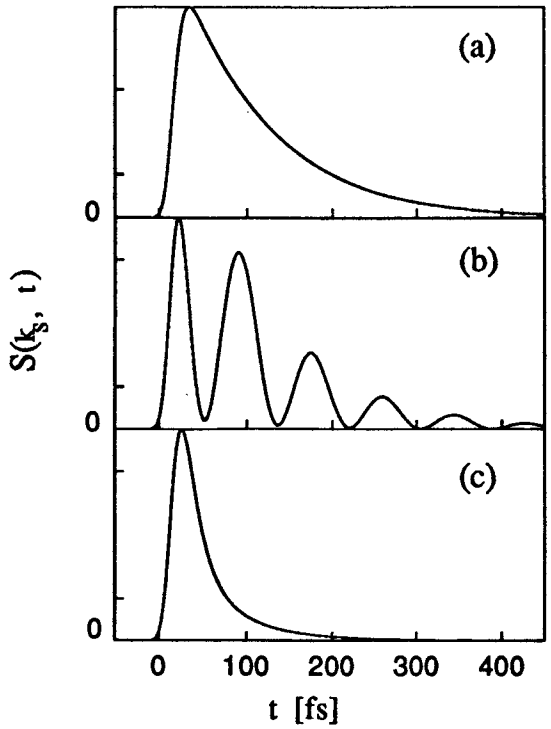

FIG. 5. Time–resolved D4FM signals of the two–band Hückel model of Polysilane for different sizes N. a) N=10; b) N=30; c) infinite size. We used resonant excitation by a 10 fs Gaussian pulse, peak Rabi frequency 0.3 meV; dephasing time $T_2 = 200fs$ and time delay $\tau = 0$.

We first examined the Hückel model for Polysilane ($\delta = 0.33$) for different sizes calculating the time-dependent D4WM signal Eq. (11). We used a short pulse excitation (which has a broad spectral width) in order to excite several band states simultaneously. For this reason we expect an oscillating structure of the time–resolved D4WM signal due to the interference of excitons with different frequencies. Fig. 5 shows the signal for zero–time delay and a transverse relaxation time of 200 fs. We excited the system on resonance (at the band edge) with a Gaussian pump pulse of 10 fs half width. The peak Rabi frequency (0.3 meV) corresponds to the low intensity limit. For small size (N=10) we recover the result of a two–level system because only the lowest level at the band edge is excited. The signal rises with the pump pulse and decays exponentially with half the transverse relaxation time. With increasing size (decreasing level spacing) oscillations can be seen with a period equal to half the level spacing of the lowest states in the two band model Fig. 5(b). The details of the signal depend crucially on parameters characterizing the excitation process. For the infinite size ($N > 100$, Fig. 5(c)) the signal is similar to the result obtained for the two–level system but the decay time is faster. In this case the continuous distribution of states within the bands acts like an inhomogeneous broadening which contributes to the dephasing in addition to the transverse relaxation time. Due to this "inhomogeneous distribution" one might expect a photon echo for negative time delays (probe proceeds the pump).[14]

The lineshape of the signal changes drastically if Coulomb interaction is taken into account, where besides the prompt peak of the free induction decay, a broad delayed component can be seen (Fig. 6). This behaviour was originally found in inorganic semiconductors like GaAs and was called interaction induced signal (IIS).[28] The origin of the IIS is the exciton–exciton interaction (terms with δn_K on the RHS of Eq. (12)). Switching off these terms the signal disappears (Fig. 6b). The position of the peak is given by the transverse relaxation time as is shown in Fig. 6a. Therefore this signal does not correspond to a usual photon echo. It originats from the scattering of the pump off the grating formed by the pump and the probe fields.

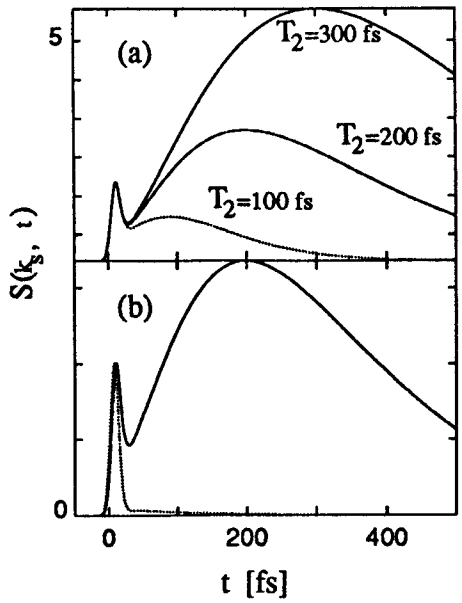

FIG. 6. Time–resolved D4WM signals for the PPP model of Polysilane for excitation at 10 meV below the lowest exciton resonance. Other parameters as in Fig. 5. a) for different dephasing times; b) with (solid) and without (dotted) exciton–exciton interaction.

VI. CHARGE BAND-LIKE EXCITONS IN C_{60}

C_{60} is a molecule with unique symmetry.[13] Its 60 carbon atoms can be described in the site representation with 5 unit cells, each of them contain 12 sites. Then the polarization can be studied by expanding of Eq. (7) in powers of the external field. In Fig. 7, we show the absorption spectra and the absolute value of the third order polarizability connected to THG ($|\gamma(-3\omega;\omega,\omega,\omega)|$). We denoted the peaks of the absorption spectra by A,B,...,F and the peaks of the dispersion of $|\gamma(-3\omega;\omega,\omega,\omega)|$ by a,b,...,j as shown in Fig. 7. $|\gamma(-3\omega)|$ is plotted versus ω and versus 3ω in order to compare the single-photon and the three-photon resonance with the linear absorption. Since the peaks a, b, c and f are at one-third the frequencies of the peaks A, B, C and F, respectively, the peaks are attributed to three-photon resonances. The peak g is at half the frequency of the peak C. Thus it is attributed to the two-photon resonance. The peaks h, i and j are at the frequencies of the peaks A, B and C, respectively. Thus they are attributed to the one-photon resonances. The frequencies of peaks d and e are a little bit lower than one-third the frequencies of the peaks D and E, respectively. However, since there are no one-photon or two-photon resonances here, they are also attributed to three-photon resonances. Meth et al. have measured the absorption and frequency dispersed THG spectra of C_{60} in thin films[30]. In the absorption, studied in the frequency range $0.41 < \omega/E_g < 1.43$, they found two closely lying resonances, the resonance with the higher frequency being more intense. In the dispersed THG studied in the frequency range $0.19 < \hbar\omega/E_g < 0.42$, they found a resonance at one-third the lower frequency but no resonance at one-third the higher frequency. These features are reproduced very well in our calculations.

The dipole moment (and hence the linear and nonlinear polarizabilities) is determined from the diagonal elements $\rho_{n,n}$, that is, the amplitude of the charge density oscillation induced by the external field at the n'th site. The sites of a C_{60} molecule lie in 8 different planes defined by $z = \pm 3.3, \pm 2.6, \pm 1.8, \pm 0.6\mathring{A}$. The number of atoms in each plane is $5, 5, 10, 10$, respectively . We consider the sum of the charges over the sites which are in the same plane because it is directly related to the total dipole moment.The total charge thus denotes a charge 'band' around C_{60} molecule at different hight z. Note that because of the symmetry of the present Hamiltonian and the stationary HF solution, all the sites with the same z-coordinate have the same time dependent charge density.

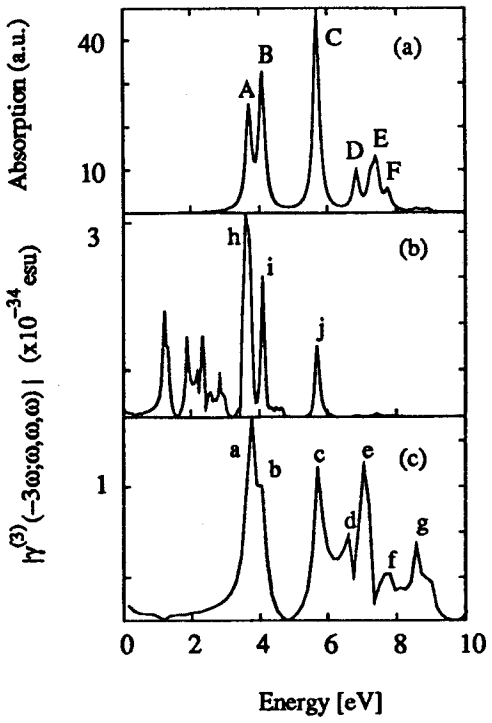

FIG. 7. (a) absorption spectra. (b) and (c) dispersion of $|\gamma(-3\omega;\omega,\omega,\omega)|$. In (a) and (b), the horizontal axis is the single photon energy ω, but in (c) the horizontal axis is 3ω.

The total charge in q'th order in the field at z induced by the external field $E(t) = E_0 \cos\omega t$ is given by

$$d_z^{(q)}(t) = \frac{1}{\sqrt{2\pi}}\{\mathrm{Re}[\tilde{d}_z^{(q)}]\cos(q\omega t) + \mathrm{Im}[\tilde{d}_z^{(q)}]\sin(q\omega t) + ...\}\,. \tag{13}$$

The total dipole moment is directly related to $d_z^{(q)}$. It can be written as

$$P^{(q)}(t) = \frac{2e}{\sqrt{2\pi}}\sum_z z\{\mathrm{Re}[\tilde{d}_z^{(q)}]\cos(q\omega t) + \mathrm{Im}[\tilde{d}_z^{(q)}]\sin(q\omega t) + ...\}. \tag{14}$$

Here we keep only terms which contribute to THG. The z dependence of the amplitude $\tilde{d}_z^{(q)}$ is shown in Fig. 8 at four different frequencies: 0.4 eV, 1.25 eV, 2.85 eV and 3.7 eV. There is no peak in the absorption and THG at 0.4 eV, no peak in the absorption but a three-photon resonance peak a in the THG at 1.25 eV, no peak in the absorption but a two-photon resonance peak g in the THG at 2.85 eV, a peak A in the absorption and a large peak h in the THG at 3.7 eV. We see from Fig. 8 that the charge densities oscillate in a very similar pattern for all frequencies in each order and amplitudes are correlated with the oscillation strength of the excitons. Thus this characteristic collective motion dominates the optics of each order. We can see two exciton like structures in each order in both the real and imaginary part. In first order, one exciton has opposite charges at $z = \pm 0.6$ Å and the other one has opposite charges at $z = \pm 3.3$ Å, and these two excitons have parallel dipole moments. A pair of opposite charges gains interaction energy with the external field when one charge is near the north pole (z is the largest) and the opposite one is near the south pole (z is the smallest) because this state has the largest dipole moment. However, since the charges are concentrated in a small region near the poles, the Coulomb repulsion energy between these charges becomes large. On the other hand, there is no significant gain of interaction energy by a pair of opposite charge near the equator ($z = 0$), but the Coulomb repulsion energy between them is smallest because these charges can spread widely near the equator. Thus these two kinds of excitons are stabilized by these two different interactions. These two interactions compete in our Hamiltonian, resulting in these two types of excitons . Consequently, the electronic structure of the

excitons and the optical response are strongly affected by the Coulomb interaction and the confinement. In second order, the first (the second) exciton has charges near the north (south) pole and opposite charges just north (south) the equator. In the third order, one exciton has opposite charges at $z = \pm 0.6\mathring{A}$ and the other one has opposite charges at $z = \pm 1.8$ and $2.6\mathring{A}$. Unlike the first order, the dipole moment of these two excitons have opposite directions in the second and third order. We have investigated $\tilde{d}_Z^{(q)}$ also at other frequencies and found that the conclusions mentioned above hold for all frequencies studied, namely, 1) there is a characteristic charge density oscillation pattern in each order and only these collective motions are excited by the external field at every frequency; 2) the magnitudes are much larger at the resonant frequencies than those at off resonant frequencies.

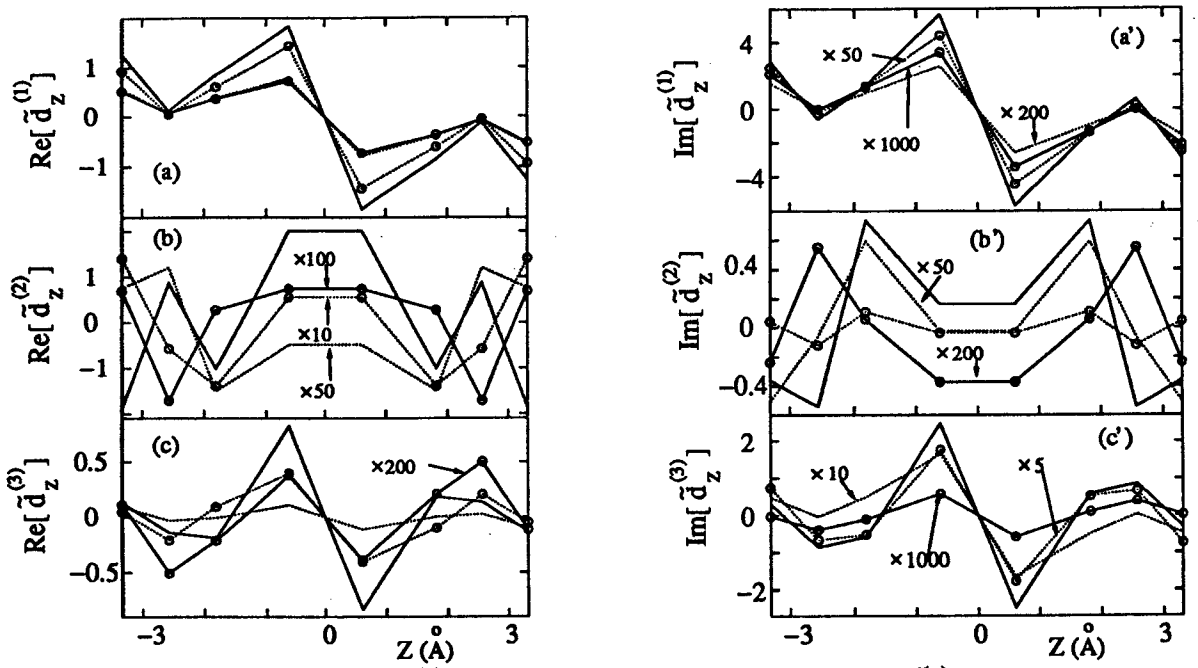

FIG. 8. The Z dependence of Re[$\tilde{d}_z^{(q)}$] (a) q=1,(b) q=2, (c) q=3 and that of Im[$\tilde{d}_z^{(q)}$] (a') q=1,(b') q=2,(c') q=3.

In the present calculation the absolute value of the polarizability at $\omega = 0.05\ eV$ is $|\gamma(-3\omega;\omega,\omega,\omega)| = 1.32 \times 10^{35}$ esu. This value is consistent with the result $|\gamma(-3\omega;\omega,\omega,\omega)| = 2.11 \sim 2.55 \times 10^{35}$ esu at $\omega = 0$ by Matsuzawa and Dixon, where the Coulomb interaction between the π electrons is taken into account.[29] However, it is more than 100 times smaller than the result $|\gamma(-3\omega;\omega,\omega,\omega)| = 2.93 \times 10^{33} esu$ at $\omega = 0$ by Harigaya and Abe, where Coulomb interaction was neglected.[16] The discrepancy can be understood as follows. First, the Coulomb interaction reduces the linear and nonlinear polarizabilities significantly. As mentioned before, exciton like charge density oscillations are responsible for the polarizabilities. Since opposite exciton charges interact attractively, the Coulomb interaction confines these charges. Furthermore, as the opposite charges separate farther, they approach the north or south poles where these charges are concentrated in small regions so that the Coulomb repulsion energy between them becomes larger. Consequently, the Coulomb interaction confines the opposite charges of the excitons by two different mechanisms: one is general and the other is characteristic of a C_{60} molecule. The confinement reduces the total dipole moment of the excitons so that the polarizabilities are reduced by the Coulomb interaction. Second, the lowest optically allowed excitation energy is 2.5 eV in their calculation but 3.7 eV in our calculation. Since the off-resonant $\gamma(0)$ is inversely proportional to the third power of the energy gap, the difference in the energy gap along accounts for a factor of 3.2 difference in $|\gamma(-3\omega;\omega,\omega,\omega)|$.

The magnitude of the off-resonant THG is important for practical devices. We now consider the factors that can yield a large off-resonant THG in π electron systems . As indicated earlier, exciton like collective motions are responsible for THG also at off-resonant frequencies, and the Coulomb interaction reduces the THG significantly by two different confinement mechanisms. We focus on the confinement mechanism which depends on the molecular structure . In the other fullerenes such as C_{70}, as the size of a molecule becomes larger, the distance between opposite charges where the charges begin to be concentrated near the poles becomes larger. Therefore weaker confinement and larger THG is expected in larger fullerenes. On the other hand, in linear chains opposite charges can separate

without being concentrated in small regions if the chain length is sufficiently long . Since the diameter of a C_{60} molecule is much smaller than the length of a linear chain consisting of 60 carbon atoms, the confinement mechanism characteristic for fullerenes does not occur in the linear chain. Therefore, for the same number of C atoms, larger THG is expected in linear chains.

In conclusion, we studied the frequency dispersed, static and time-resolved third order nonlinearity of conjugated systems. Our calculations clearly demonstrate the uncorrelated nature of the electron and the hole in the Hückel model, and how the Coulomb attraction of the electron-hole pair changes the nature of the elementary excitations which closely resemble charge-transfer (intermediate) excitons. Additionally, the anharmonic oscillator framework provides a real-space picture for the nonlinearity and thus yields a physical and intuitive insight. We studied the temporal profile of the time–resolved D4WM signal of Polysilane for excitation with intense ultrashort laser pulses. In the Hückel model the coupling of several interband states by ultrashort pulses leads to oscillations in the signal which correspond to the level spacing. For infinite size we obtained a photon echo like behaviour. The Coulomb interaction generates beside the free induction decay a broad delayed component which is collective in nature and cannot be interpreted as an photon echo. Many–body effects such as band gap renormalization come into play for high intensity excitation showing up in the signal. Exciton like characteristic collective motions are excited by the external field in C_{60}. These excitons are very similar in shape in each order of the field and for all frequencies which we have investigated. The magnitudes of these collective motions strongly depend on the frequencies.

ACKNOWLEDGMENTS

The support of the the Air Force Office of Scientific Research and the NSF Center for Photoinduced Charge Transfer, is gratefully acknowledged.

---

[1] *Nonlinear Optical Properties of Organic Molecules and Crystals*, edited by D. S. Chemla and J. Zyss (Academic, Orlando, 1987), Vol. I and II.
[2] S. Etemad and Z. Soos,in *Spectroscopy of Advanced Materials*, Edited by R.J.H. Clark and R.E. Hester, Wiley, N.Y. (1991).
[3] W.E. Torruellas, K.B. Rochford, R. Zanoni, S. Aramaki and G.I. Stegeman, Opt. Comm. 82, 94 (1991).
[4] W.-S. Fann, S. Benson, J. M. Madey, S. Etemad, G. L. Baker and F. Kajdar, Phys. Rev. Lett. 62, 1492 (1989); P.D. Townsend, W.-S. Fann, S. Etemad, G.L. Baker, Z.G. Soos and P.C.M McWilliams Chem. Phys. Lett. 180, 485 (1991).
[5] J.P. Herrmann and J. Ducuing, J. Appl. Phys. 45, 5100 (1974); P. Agrawal, C. Cojan, and C. Flytzanis, Phys. Rev. B 17, 776 (1978).
[6] Z. Shuai and J.L. Bredas, Phys. Rev. B 44, 5962 (1991).
[7] J.R. Heflin,K.Y. Wong, O. Zamani-khamiri and A.F. Garito, Phys. Rev. B. 38, 1573 (1988); Mol.Crys. Liq. Crys. 160, 37 (1988).
[8] S. Mukamel and H.X. Wang, Phys. Rev. Lett. 69, 65 (1991).
[9] H.X. Wang and S. Mukamel, Nonlinear Optics, in press.
[10] S. Mukamel and H.X. Wang, in Optics of Semiconductor Nanostructures, editors F. Henneberger amd S. Schmitt–Rink, 1992, (Academie Verlag,Berlin ,1993).
[11] H.X. Wang and S. Mukamel, Chem. Phys. Lett. 192, 417 (1992).
[12] H.X. Wang and S. Mukamel, J. Chem. Phys. 97, 8019 (1992).
[13] A.Takahashi, H.X.Wang and S. Mukamel, to be published.
[14] M. Hartmann and S. Mukamel, to be published in J.Chem. Phys.
[15] Z.H. Kafafi, J.R. Lindle,R.G.S. Pong,F.J. Bartoli, L.J. Lingg and J. Milliken, Chem. Phys. Lett. 188, 492 (1992); W.J. Blau, H.J. Byrne, D.J. Cardin, T.J. Dennis, J.P. Hare, H.W. Kroto, R. Taylor and D.R.M. Walton, Phys. Rev. Lett. 67, 1423 (1991); R.J.Knize and J.P. Partanen, Phys. Rev. Lett. 68, 2704 (1992).
[16] K. Harigaya and S. Abe, Japan J. Appl. Phys. 31, L887 (1992). S. Abe, M. Schreiber, and W.P. Su and J. Yu, Phys. Rev. B 45, 9432 (1992–II); S. Abe, J. Yu, and W.P. Su, Phys. Rev. B 45, 8264 (1992–I).
[17] B. E. Kohler, J. Chem. Phys. 93, 5838 (1990).

[18] M. Cho, N.F. Scherer, G.R. Fleming, and S. Mukamel, J. Chem. Phys. 96, 5618 (1992).
[19] S. Abe, M. Schreiber, and W.-P. Su, Chem. Phys. Lett. 192, 425 (1992).
[20] D. Yaron and R. Silbey, Phys. Rev. B., 45,11655 (1992).
[21] P.Ring and P. Schuck, The Nuclear Many-Body Problem, (Springer-Verlag, New York, 1980).
[22] J.R. Kuklinsky and S. Mukamel, Phys. Rev. B 42, 295 (1990).
[23] V. Langer, H. Stolz, and W. von der Osten, Phys. Rev. Lett. 64, 854 (1990).
[24] M.Hartmann and W. Schäfer, in proceedings of the conference on "Nonlinear Optics of Excitons in Confined Systems", Naxos (Sicily), Sept. 1991, p. 200.
[25] W.B. Bosma and S. Mukamel, B.I. Greene, S. Schmitt–Rink, Phys. Rev. Lett. 68, 2456 (1992).
[26] G. Noll, U. Siegner, S. Shevel, and E. Göbel, Phys. Rev. Lett. 64, 792 (1990).
[27] J.A. Leegwater, L.E. Fried, and S. Mukamel, Z. Phys. D., to be published in 1993.
[28] W. Schäfer and F. Jahnke, Phys. Rev. B, to be published.
[29] N. Matsuzawa and D.A. Dixon, J. Chem.Phys. 96, 6241 (1992).
[30] J.S. Meth, H. Vanherzeele and Y. Wang, Chem. Phys. Lett. 197, 26 (1992).
[31] H. Hoshi, N. Nakamura, Y. Maruyama, T. Nakagawa, S. Suzuki, H. Shiromaru and Y. Achiba, Japan J. Appl. Phys. Letters, 30, L1397 (1991).
[32] M. Lindberg, R. Binder, and S. Koch, preprint.